nature protocols

https://doi.org/10.1038/s41596-024-01125-5

Protocol

Check for updates

Laser microsurgery for presynaptic interrogation

Hovy Ho-Wai Wong [1,2,3] ✉, Alanna J. Watt [4] & P. Jesper Sjöström [1] ✉

Abstract

Synaptic connections among neurons are critical for information processing and memory storage in the brain, making them hotspots for neuropathologies. Understanding the physiology of synapses, therefore, may facilitate the development of therapeutic approaches. However, synapses are micrometer-sized functional structures involved in many neuronal processes, where the challenge is deciphering differential signaling in presynaptic and postsynaptic compartments of relatively intact microcircuits. Here we developed a method combining two-photon laser microsurgery with compartment-specific electrophysiological activation and readout to improve the specificity with which neuronal signaling is detected. After finding a connection, femtosecond laser pulses are used to sever the presynaptic axon from the cell body with micrometer precision. This microdissection method is effective to a depth of at least 100 µm. The initial segment of the isolated axon is extracellularly stimulated and activated to release neurotransmitters, as detected via a recipient whole-cell neuron, which is being recorded. This methodology is an alternative to axonal patch-clamp recordings, which are short-lasting and difficult. Together with pharmacology and genetic manipulation, our approach allows the interrogation of compartmentalized signaling in intact synapses. The total time of laser exposure is a few seconds and the microsurgery takes 5–10 min, which enables the interrogation of multiple synapses within an experiment. Our protocol provides a tool to investigate compartment-specific signaling in relatively intact brain tissue, enabling a more comprehensive understanding of neuronal synapses.

Key points

- A two-photon laser microsurgical procedure where femtosecond laser pulses are used to sever the presynaptic axon from its cell body, enables testing neurotransmission across a synapse in a whole neuron which is being recorded.
- The microdissection method is an alternative to patch-clamp recordings of axons and can be performed up to a depth of 100 µm providing an approach to studying neurotransmission across neuronal synapses in a compartment-specific manner in relatively intact brain tissue.

Key reference

Wong, H. H. et al. *Neuron* **112**, 264–276.e266 (2024): https://doi.org/10.1016/j.neuron.2023.10.011

[1]Centre for Research in Neuroscience, Brain Repair and Integrative Neuroscience Program, Department of Neurology and Neurosurgery, Department of Medicine, The Research Institute of the McGill University Health Centre, Montreal General Hospital, Montreal, Quebec, Canada. [2]School of Biomedical Sciences, The Chinese University of Hong Kong, Hong Kong, China. [3]Gerald Choa Neuroscience Institute, The Chinese University of Hong Kong, Hong Kong, China. [4]Biology Department, McGill University, Montreal, Quebec, Canada. ✉e-mail: hovy.wong@cuhk.edu.hk; jesper.sjostrom@mcgill.ca

Introduction

Neuronal connections—or synapses—are micrometer-sized contact points between brain cells. They are important for rapid information transfer and memory storage. It has been estimated that each neuron forms thousands of synapses[1–3]. With the numerous synapses buried in a dense network of neuronal processes and cells, teasing apart the differential contribution of presynaptic and postsynaptic regulation has been an enduring challenge.

As the postsynaptic cell is commonly used as the experimental readout, it is tempting to interpret synaptic changes as arising in the measured postsynaptic cell or compartment[4]. This can lead to the view that the axon has a relatively passive role in regulating synaptic changes. Yet, just like the signal-receiving postsynapse may influence neurotransmission, so can the signal-producing axon. For instance, long-term synaptic plasticity can be induced both pre- or postsynaptically[5], as well as being induced postsynaptically while being expressed presynaptically[4]. Examining the role of presynaptic regulation will, therefore, provide a more comprehensive understanding of synapse health and disease[6–10].

Our understanding of the presynapse has been hampered by the complications of discerning pre- versus postsynaptic effects at intact synapses. Strategies for manipulating submicron-thick axons have also been scarce. Therefore, researchers have often relied on indirect methods, such as analysis of the coefficient of variation (CV) or paired-pulse ratio (PPR)[4,11], but these can sometimes be inconclusive[11]. Here, we showcase a method that relies on laser microsurgery and electrophysiology to directly uncover presynaptic signaling. This protocol was developed with mouse brain tissue but could in principle be applied to tissue from rats, nonhuman primates or even humans.

Development of the protocol

Protein synthesis has been linked to memory for over 60 years[12], with the prevalent view that the newly synthesized proteins originate in the cell body[13] or the dendrites[14,15]. Yet, using intracellular drug loading to selectively target the pre- but not postsynaptic cell, we found that protein synthesis in the presynaptic cell sustains neurotransmission[16]. This was surprising because basal neurotransmission has been widely believed to be independent of protein synthesis. We resolved this conundrum by revealing that high- but not low-frequency neurotransmission triggers translation-dependent synaptic release[16]. To discern whether presynaptic protein synthesis in the somatodendritic or axonal compartment is important in high-frequency neurotransmission, a method to separate their contributions was needed.

One way is to perform axotomy, by physically severing the axon from the somatodendritic compartment. However, axons and dendrites are often intermingled, rendering precise surgical procedures difficult. To address this problem, we developed a laser microsurgery protocol to perform axotomy with micrometer precision[16]. Combining with targeted stimulation of the isolated axon, our protocol offers an efficient pipeline to analyze compartment-specific signaling.

Application of the method

We utilized our protocol for testing the contribution of local protein synthesis in axons with intact synapses[16]. With genetic manipulations or pharmacological reagents, this method can be directly used for examining virtually any signaling in axons in the context of neurotransmission. The ability to perform precise optical microsurgery maximally preserves the local tissue. In our experience, the longevity of electrophysiology recordings with this method is on par with whole-presynaptic-cell recordings, that is, typically over an hour (67 ± 6 min after axotomy, $n = 8$). This timeline allows drug application to interrogate molecular pathways. Moreover, although not experimentally tested by us, adaptation of this protocol is anticipated to be broadly useful for other biology questions, as discussed below.

Similar to basal neurotransmission, long-term plasticity paradigms[17], such as spike-timing dependent plasticity or burst stimulation, can be examined. This two-photon

laser microsurgery method can also be easily adapted to look at axon degeneration and regeneration[18]. With the capability to sever axons deeper than 100 µm, the procedure is anticipated to work in a wide range of models.

To bypass the need for whole-cell recordings, biosensors are emerging to be instrumental in measuring neurotransmitter release, such as iGluSnFR[19,20] for glutamate and iGABASnFR[21] for GABA (γ-aminobutyric acid). Expressing genetically encoded calcium sensors[22] would allow the abolishment of evoked antidromic action potentials to be monitored in the presynaptic cell, providing an indicator that the axon is successfully isolated from the cell soma for optimization. By simultaneously expressing an opsin, an all-optical method to confirm axon isolation is possible, for example, in the combination of channelrhodopsin-2 and a 473-nm laser[23].

Besides experiments with mature axons that have already formed synapses[16,24], our optical axotomy protocol may also be used to explore axon development. Examples include axon navigation, fasciculation, branching and topographical mapping[25–28].

Comparison with other methods

The idea of isolating neuronal processes to examine their autonomy can be traced back nearly 100 years[29]. Many protocols involved the use of preparations in vitro[18,29–32], which offers the ease of performing surgical cuts. Ex vivo and in vivo preparations with well-stratified neuronal processes have also been used, such as hippocampal CA1 apical dendrites[13–15], the optic nerve[25,28,33,34] and cerebellar Purkinje cell axons[24]. The relatively pure neuronal process mass permits a macroscopic cut to sever the whole process mass. However, in most parts of the central nervous system, neuronal processes are not organized in clear bundles. In the neocortex, for instance, even unconnected axons and dendrites often traverse each other, making macroscopic cuts infeasible. Moreover, due to sparse connectivity rates (for example, ~11% between pyramidal cells[35]), the presence of connections can only be revealed after patching the cells. This means targeting specific neuronal processes for severing before patching[13–15] is not possible, while performing a surgical cut after finding connections would disrupt the patched cells. Together, these call for a precise microsurgery method. Previous protocols have demonstrated that laser microsurgery is effective for single axon lesions to study axon regeneration and degeneration[36,37]. Here, we present an optimized two-photon laser-surgery protocol that provides real-time readout of axotomy success, thereby minimizing laser exposure. The absence of tissue perturbation permits sensitive methods such as whole-cell patch clamp recordings to be simultaneously used.

Isolating the axon means it can no longer be triggered by the presynaptic patch electrode. To sample neurotransmission, the isolated axon must, thus, be directly stimulated some other way. A powerful method to achieve this is single axon patching. However, this is only feasible in systems with large presynaptic boutons. For example, boutons of hippocampal mossy fiber[38,39] and the calyx of Held[40] can in mammals be 5–10 µm in diameter, whereas those of neocortical pyramidal neurons are typically smaller than 1 µm. In addition, bouton patch-clamp recordings are challenging[38,39] and short-lasting[41], limiting their utility.

An alternative method is extracellular stimulation, which is easy to implement but can inadvertently excite multiple inputs. This signal contamination can confound results as connection properties are often specific to both the pre- and postsynaptic cell types or synapse-type specific[42,43]. To overcome this, we developed targeted axon stimulation that relies on minimal stimulation of the axon, providing a spatial tolerance of ~2 µm to ensure specificity.

Experimental design

Finding connection

The experiment begins with finding a connection between the cells of interest (Fig. 1). Although paired recordings with dual-patch would suffice, we recommend multiple patch-clamp recordings, because it increases the yield of connections[44]. To visualize neuronal processes of the patched cells, different fluorescent dyes are added in each pipette (Fig. 2). As many imaging systems only have two photomultiplier detectors, mixing two dyes in different concentrations across patched cells effectively extends the color palette[16,44] (Fig. 2).

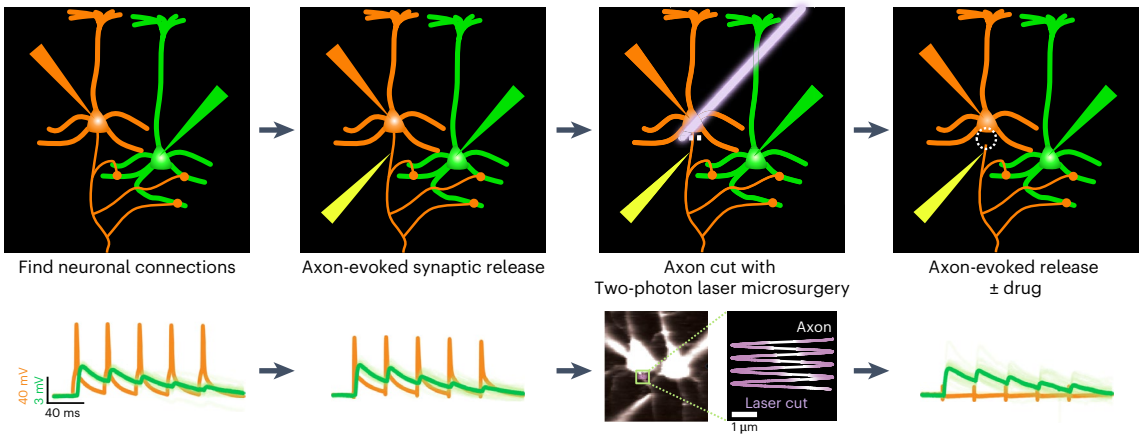

Fig. 1 | Overview of targeted axon stimulation combined with two-photon laser axotomy. Axonal stimulation (yellow) after two-photon laser axotomy enables testing the specific role of axonal protein synthesis in evoked release. Left: soma-evoked action potentials (orange) and postsynaptic responses (green). Axon-evoked action potentials and postsynaptic responses before (middle) and after (right) axotomy. Images showing the 4 µm × 2 µm sine-square scan (purple) used to cut the axon. After axotomy, axon-evoked release can continue to be used for assessing neurotransmission, with or without pharmacology.

Establishing targeted axon stimulation

Guided by two-photon imaging, a dye-filled stimulation pipette is positioned adjacent to the proximal axon stretch ~20 µm from the cell body (Fig. 1). Suprathreshold axonal stimulation generates action potentials that travel down the axon to elicit neurotransmitter release at presynaptic terminals. This is recorded as postsynaptic responses in connected neurons. Additionally, action potentials also travel antidromically to the cell body. This signal is captured by the patch pipette of the presynaptic cell body. By applying stimulation voltage steps, the firing threshold can be determined by the antidromic action potentials.

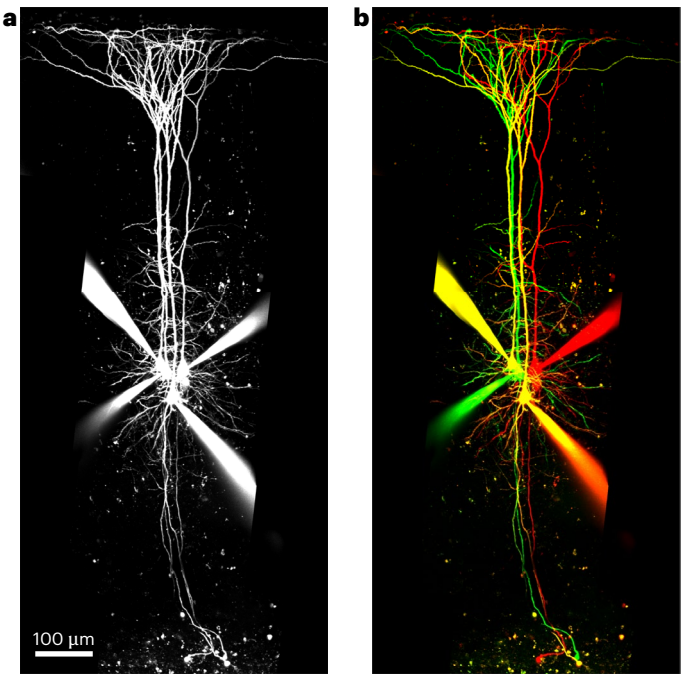

Fig. 2 | Multicolor imaging aids identification of neuronal processes. Neurons have numerous neuronal processes, making it hard to find the axon of interest for axotomy. **a**, With single-color imaging, the cell morphologies blend together and are hard to distinguish. **b**, By contrast, multicolor imaging allows rapid identification of individual neurons and their processes.

Two-photon laser axotomy

After establishing stable axon stimulation, the two-photon imaging system is focused on the axon stretch ~5–10 µm from the cell body. While monitoring the antidromic responses of the presynaptic cell, a 500-ms-long laser cut is performed once every 10 s (Fig. 1). Successful axotomy is indicated by the attenuation of antidromic responses and other cell property changes, detailed in the 'Procedure' section below.

Electrophysiology recording of connection with isolated axon

The antidromic and postsynaptic responses are continuously monitored after axotomy. The recording typically takes ~15 min to recover and stabilize. Following this, the recording with the isolated axon can be made with or without manipulations, such as pharmacological manipulation (Fig. 1). Forms of analysis such as PPR and CV can further help to confirm pre- versus postsynaptic locus of changes[11,16].

Expertise needed to implement the protocol

A key technique for implementing this protocol is paired recording, which is not strictly a requirement for axotomy but rather one for finding connected pairs of neurons. Although paired recording is an advanced electrophysiology technique, we routinely transfer this knowledge to undergraduate trainees in weeks to months[44], and trainees typically learn two-photon imaging even faster. All in all, laser axotomy is relatively accessible compared with other axon interrogation techniques, such as axonal patch clamp[38–40]. The typical user of this technique would be graduate students and postdocs with a foundational background in microscopy and electrophysiology.

Limitations

The physical stability of the combined patch-clamp/imaging rig is crucial to achieve specific axonal stimulation, since vibrations might disrupt recordings. Work should, therefore, be carried out on a setup with an air table, to minimize vibrations.

As with other types of electrophysiology experiment, cell health is key to successful recordings[45].The procedure of this protocol is lengthy, so it is important to continuously monitor cell health indicators online, such as membrane potential and input resistance[44,45]. Consistent application of selection criteria across conditions ensures an unbiased high-quality dataset. Yet, as for extracellular or optogenetic stimulation, health indicators are not readily available for presynaptic axons severed from their somata. Control conditions, for example, without drugs, provide a solution to this limitation.

This protocol was developed for finding axons of excitatory pyramidal cells, which have distinct morphological features to aid axon identification in the neocortex. Therefore, additional development might be needed to adapt this to presynaptic interrogation of inhibitory synapses.

While laser axotomy may help discern pre- versus postsynaptic signaling when combined with, for example, judicious pharmacological manipulations, it should ideally be combined with other methods. For instance, analyses of presynaptic changes such as PPR and CV can help ascertain the locus of expression of effects such as long-term plasticity[11]. Another experiment to help localize effects is to intracellularly dialyze drugs into the pre- or the postsynaptic cell[16]. Moreover, direct imaging of vesicle release with Fei Mao dyes[16,34], synaptopHluorin[46] or neurotransmitter biosensors[19] powerfully complements laser axotomy. Combining different approaches, thus, offers a powerful complementarity for pre- versus postsynaptic interrogation.

Regulatory approvals

Apart from the typical standard operation protocols needed for animal work and laser usage, no additional regulatory approvals were required specifically for this protocol.

Materials

Reagents for cell and pipette visualization

- Alexa Fluor 488 hydrazide (Invitrogen, cat. no. A10436)
- Alexa Fluor 594 hydrazide (Invitrogen, cat. no. A10438)

Reagents for artificial cerebrospinal fluid (ACSF)

- NaCl (Thermo Fisher Scientific, cat. no. S271-3)
- KCl (Sigma-Aldrich, cat. no. P3911)
- $NaH_2PO_4 \cdot H_2O$ (Sigma-Aldrich, cat. no. 71507)
- $NaHCO_3$ (Sigma-Aldrich, cat. no. S6297)
- $MgCl_2$ hexahydrate (Sigma-Aldrich, cat. no. M2670)
- $CaCl_2$ dihydrate (Sigma-Aldrich, cat. no. 223506)
- D^+-glucose (Sigma-Aldrich, cat. no. G8270)
- Double-distilled water (ddH_2O; from MilliQ Direct Water Purification System, Millipore Sigma, cat. no. C85358)

Reagents for gluconate-based internal solution

- KCl (Sigma-Aldrich, cat. no. P3911)
- K-gluconate (Sigma-Aldrich, cat. no. G4500)
- HEPES buffer (Sigma-Aldrich, cat. no. H3375)
- Mg–ATP (Sigma-Aldrich, cat. no. A9187)
- Na-GTP (Sigma-Aldrich, cat. no. G8877)
- Na–phosphocreatine (Sigma-Aldrich, cat. no. P7936)
- KOH (Supelco, cat. no. 1.09108)
  ▲ **CAUTION** KOH is corrosive, which can cause severe skin burns and eye damage.
- Sucrose (Sigma-Aldrich, cat. no. S0389)
- Optional: biocytin (Sigma-Aldrich, cat. no. B4261)
- ddH_2O (From MilliQ Direct Water Purification System, Millipore Sigma, cat. no. C85358)

Other reagents

- 6% Sodium hypochlorite solution; household bleach (Clorox Original Concentrated Bleach)
  ▲ **CAUTION** Sodium hypochlorite is corrosive, which can cause severe skin irritation and serious eye damage.

Animals

- Mice (C57BL/6J breeder mice were purchased from The Jackson Laboratory. The mice were group housed in a standard 12 h light–dark cycle. All animal procedures conformed to the Canadian Council on Animal Care as overseen by Montreal General Hospital Facility Animal Care Committee, with appropriate licenses. Male or female postnatal day 11–16 mice were anesthetized with isoflurane and sacrificed once the limb withdrawal reflex was absent. No sex differences were found in the time required for laser axotomy (male: 3.65 ± 1.0 s, $n = 15$ versus female: 5.27 ± 1.9 s, $n = 24$; $P = 0.41$))
- This procedure could in principle be applied without amendments to brain tissue from other species, such as rats[35], nonhuman primates[47] or even humans[48]
  ▲ **CAUTION** All experiments must be performed in accordance with relevant institutional and national guidelines.

Equipment for electrophysiology

- Nylon syringe filters—4 mm diameter, 0.2 µm pore size (VWR, cat. no. 28196-050)
- Osmometer (Advanced Instruments, cat. no. Osmo1)
- Standard-wall borosilicate capillaries—1.5 mm outer diameter, 0.86 inner diameter (Harvard Apparatus, cat. no. G150F-4 or Sutter Instrument, cat. no. BF150-86-10)

- Micropipette puller (Sutter Instrument, cat. no. P-1000)
- Silver wires for recording electrodes—0.25 mm diameter (Harvard Apparatus, cat. no. 64-1319)
- Silver wires for recording electrodes—0.37 mm diameter (Harvard Apparatus, cat. no. 64-1320)
- Biphasic Stimulus Isolator (Dagan, cat. no. BSI-950)
- BX51WI microscope frame (Olympus)
- PatchStar micromanipulator system (Scientifica)
- Motorized movable top plate (Scientifica)
- Plan N 4×/0.10 objective (Olympus, cat. no. N1215700)
- LUMPlanFL N 40×/0.80 objective (Olympus, cat. no. N2667700)
- MultiClamp 700B amplifiers (Molecular Devices)
- PCI-6229 (cat. no. 191332B-01) or PCIe-6323 (cat. no. 781045-01) data acquisition and control boards (National Instruments)
- Resistive inline heater (Scientifica, cat. no. SM-4500)

Equipment for two-photon laser microscopy

- MaiTai HP titanium-sapphire laser (Spectra-Physics)
- Shutter-controller pair for gating laser (Thorlabs, cat. no. SH05 and SC10)
- Polarizing beam splitter and half-wave plate for manual laser attenuation (Thorlabs, cat. no. GL10-B and AHWP05M-980)
- Laser power meter (Thorlabs, cat. no. PM100A and S121C)
- BX51WI microscope frame (Olympus)
- 3-mm Galvanometric mirrors (Cambridge Technology, cat. no. 6215H, or Pangolin Laser Systems ScannerMAX Saturn 1B 56S with MacDSP)
- Plan N 4×/0.10 objective (Olympus, cat. no. N1215700)
- LUMPlanFL N 40×/0.80 objective (Olympus, cat. no. N2667700)
- Dichroic mirror for fluorescence collection (Semrock, cat. no. FF665-Di01 or FF695-Di01A)
- Infrared-blocking filter (Semrock, cat. no. FF01-680/SP-25)
- Dichroic mirror for splitting green/red fluorescence (Semrock, cat. no. FF560-Di01)
- Emission filter for green fluorescence collection (Chroma, cat. no. ET525/50m)
- Emission filter for red fluorescence collection (Chroma, cat. no. ET630/75m)
- R3896 bialkali photomultiplier tubes (Hamamatsu)
- Laser-scanning Dodt contrast detector (Thorlabs, cat. no. PDA100A-EC)
- PCI-6110 (cat. no. 777475-01) or PCIe-6374 (cat. no. 785817-01) data acquisition and control boards (National Instruments)

Reagent setup

Preparation of external solution, ACSF

A 10× concentrated stock is prepared and stored at 4 °C for up to 1 month. To make 10× ACSF, dissolve 1.25 M NaCl, 25 mM KCl, 12.5 mM NaH_2PO_4 and 260 mM $NaHCO_3$ in ddH_2O. On the experiment day, dilute the 10× stock to 1× with ddH_2O. Typically, 1–2 L of 1× ACSF is recommended per experiment day for both brain slicing and patching. The 1× bicarbonate-based ACSF is then bubbled with carbogen (95% O_2/5% CO_2) to stabilize the pH at ~7.4 and to ensure proper oxygenation. Effective carbogen diffusers may be made with aquarium equipment. To complete the solution, 1 mM $MgCl_2$ and 2 mM $CaCl_2$ are added. For mouse neurons, adjust the osmolality to 338 ± 1 mOsm/kg by adding D-glucose. For rat, adjust the osmolality to 319 ± 1 mOsm/kg.

▲ **CRITICAL** $MgCl_2$ and $CaCl_2$ are prone to precipitation at basic pH, which renders the ACSF milky white instead of colorless. $MgCl_2$ and $CaCl_2$ should hence be added after bubbling with carbogen for >5 min to allow pH stabilization.

▲ **CRITICAL** Osmolality is crucial for maintaining neuronal health and forming long-lasting whole-cell patch clamp recordings.

▲ **CRITICAL** Despite 1× ACSF can be kept at 4 °C for a few days (with cap on to prevent CO_2 outgassing and precipitation), it is highly recommended to prepare fresh 1× ACSF on each experimental day. This avoids microbial growth and changes in osmolality.

Preparation of gluconate-based internal solution

A stock is prepared and stored at −20 °C for up to 1 year. First, prepare a 1 M HEPES buffer with ddH_20 and calibrate to pH 7.4 with 1 M KOH solution. As HEPES is a good buffer and would require a considerable volume of KOH to reach pH 7.4, add ddH_20 to only ~80% of the final volume when making the 1 M HEPES and top up to 100% after pH calibration. Next, dissolve 5 mM KCl and 115 mM K-gluconate in ddH_2O to ~90% of final volume, followed by adding 10 mM HEPES from the 1 M solution. This solution mix is then calibrated to pH 7.2 with 0.5 M or 1 M KOH. To complete the solution, dissolve 4 mM Mg–ATP, 0.3 mM Na–GTP and 10 mM Na–phosphocreatine. If postexperiment cell morphometry is intended, 0.1% weight/volume biocytin can also be added for histology. This mixture is then sonicated for ~30 min and adjusted to pH 7.2–7.4 with 1 M KOH. For mouse neurons, adjust the osmolality to 310 ± 1 mOsm/kg by adding sucrose. For rat neurons, adjust the osmolality to 294 ± 1 mOsm/kg. The solution should then be aliquoted for freezing. A 400 µL aliquot is typically ample for one experiment day.

▲ **CRITICAL** For internal solution, it is important to calibrate pH with KOH instead of the commonly used NaOH. This is because addition of NaOH would disrupt the sodium ion reversal potential. By contrast, addition of KOH does not appreciably change the potassium ion reversal potential as the concentration is already relatively high.

▲ **CRITICAL** HEPES produces hydrogen peroxide when exposed to ambient light. HEPES stock solution should, therefore, be shielded from light and made fresh every time when a new batch of internal solution is made. We found that few-months-old HEPES stock solution can lose its pH buffering capacity.

▲ **CRITICAL** ATP and GTP provide energy sources for the recorded cell. However, these chemicals are prone to degradation. Therefore, internal solutions should be aliquoted and frozen at −20 °C after being made. Each aliquot should only be thawed once and be disposed of at the end of each experiment day.

▲ **CRITICAL** Osmolality is crucial in maintaining neuronal health and forming long-lasting whole-cell patch clamp recordings. Cells are particularly sensitive to the quality of internal solution as the cells are dialyzed with the internal solution.

On each experiment day, thaw an aliquot at room temperature. Vortex and spin down the tube to ensure the osmolality is not affected by vaporization. Add the desired dyes and/or drugs into the solution and sonicate. The osmolality should then be measured again and adjusted, if necessary. To avoid clogging of patch pipettes, the internal solution is filtered. We found that the 4 mm diameter syringe filters with 0.2 µm pore size work well for general purposes. These filters have a small footprint and can be directly attached to the syringe tip. They, therefore, result in less dead volume, which may be particularly important for precious reagents.

▲ **CRITICAL** Filter membranes are commonly made of nylon or cellulose acetate, which some chemicals may adhere to. For instance, nylon membrane tends to retain proteins, so peptide-based inhibitors are not compatible. Instead, polyvinylidene difluoride membrane is preferable.

Addition of fluorescent dyes to the solution

When recording and dye-filling multiple cells simultaneously, the origin of neuronal processes can be hard to tell apart. In addition, for best real-time feedback to the experimenter, it is desirable for the target axon and axon stimulation pipette to be easily distinguished. To aid identification, fluorescent dyes may be added to solutions. Alexa Fluor 488 and 594 hydrazide dyes typically work well on most green/red dual-color imaging systems, although this depends on the precise choice of filter sets. These dyes are bright, nontoxic at broad concentration range, and spectrally separated for emission collection. In our experience, Alexa Fluor 594 is brighter and can hence be used at lower concentrations. To enable visualization of micrometer-sized neuronal processes, we recommend using Alexa Fluor 488 at 100 µM and Alexa Fluor 594 at 50 µM. To extend the color palette, using mixtures of these two dyes is an affordable and easily implementable option[16]. For instance, mixing 100 µM Alexa Fluor 488 with 25 µM Alexa Fluor 594 results in more yellow color and mixing 60 µM Alexa Fluor 488 with 50 µM Alexa Fluor 594 gives more orange color (Fig. 2). Note that the axon stimulation pipette must be filled with ACSF and not internal solution; hence, care should be taken to avoid mixing up solutions for patching.

Preparing acute brain slices

Brain extraction

Mouse is anesthetized with isoflurane, as tested by absent limb withdrawal reflex, which should take 1–2 min. The mouse is quickly decapitated with a pair of sharp scissors. By holding the head with the thumb and index finger on the two lateral sides and middle finger underneath, the skin overlying the skull is cut open with small surgical scissors by following the brain midline. To expose the skull, the two skin flaps are flipped to the sides such that the thumb and index finger now also hold the skin. Next, the occipital bones lateral to the cerebellum are cut by inserting a pair of small scissors at the junction where the spinal cord and cerebellum meets. This is followed by a cut of the skull along the midline of brain until the olfactory bulb is exposed and then lateral cuts of the skull at the junction of the olfactory bulb and cerebral cortex. The skull can then be lifted and pulled laterally with forceps. This procedure exposes the brain with minimal damage. With a spatula, the brain is detached from the brain and placed in a beaker with ice-cold ACSF bubbling with carbogen.

Brain slicing

The brain is dissected in cold ACSF to extract the tissue block of interest. To stably mount the brain tissue block to the slicing stage, a moderate amount of cyanoacrylate glue is applied on the platform. By using an angled spatula, transfer the tissue to platform. This tissue block should be blotted briefly with filter paper to remove excess ACSF. The assembly is then mounted to the vibratome. Using a chiller to keep the cutting solution at <4 °C is recommended. We have had good results with 0.12–0.15 mm/s slicing speed for 300 µm brain slices. For details, please refer to previous guides[44,45].

Equipment setup

Microscope

Two-photon microscope setups vary across labs. Here, we chiefly relied on a basic setup custom-built from the Olympus BX51WI microscope frame. We have also used two-photon microscopes based on Scientifica's Slicescope, with either epi- or substage detectors, with comparable results. These designs are described in the Extended Data Fig. 1. We fully expect that other two-photon imaging setups would be similarly efficacious for laser axotomy, provided the same laser power and similar objective. It is, however, advisable to calibrate the procedures to account for differences across setups.

Our protocol used a galvo–galvo scanner system and was not tested with a resonant scanner. Since resonant scanners operate with reduced dwell time and minimal photodamage, such systems may not be ideal for two-photon laser microsurgery. However, many commercial resonant-scanner setups allow for switching to galvo-only scanning mode.

Hardware setup for electrophysiology-triggered laser axotomy

To ensure synchronization, the data acquisition and control boards must be wired up so that one triggers the other. The precise wiring strategy differs for different boards and software. In our case, the imaging board (NI PCI-6110 or PCIe-6374) was triggered by the electrophysiology board (NI PCI-6229 or PCIe-6323).

Software for electrophysiology

Commercial software packages can be used for multiple whole-cell recording, including AxoGraphX (AxoGraph), Igor Pro (WaveMetrics), MATLAB (MathWorks) and pCLAMP (Molecular Devices). Igor Pro and MATLAB employ scriptable analysis workspaces, which need software scripts such as ePhus and NeuroMatic. Our in-house software, Multipatch, implemented in Igor Pro is available on GitHub via https://github.com/pj-sjostrom/MultiPatch. We detail software and hardware solution in another guide[44].

Fabricating micropipettes

For multiple whole-cell recording experiments in current clamp, fabricate pipettes with pipette resistance of 5–6 MΩ. It helps to shape micropipettes so that they have relatively thin shank, because this design disrupts the tissue less, which is particularly favorable when patching

multiple cells. In addition, high pipette resistance generally implies small pipette tip diameter, which in turn promotes the formation of gigaohm seals. Although the pipette resistance is a key determinant of series resistance, current clamp experiments are less sensitive to signal distortions caused by series resistance. However, voltage-clamp experiments can be distorted by high series resistance, which is why 2–4 MΩ pipettes are typically preferable in this scenario. For a more detailed discussion, please refer to established guides[44,45].

Conditioning silver electrodes

For recording electrodes, straighten the portion that is inserted into the micropipettes to prevent electrode surface from being scraped off. For ground electrodes, use flat, unserrated forceps to remove the salt deposits on the surface. Next, coat the silver ground and recording electrodes in 6% sodium hypochlorite solution, such as household Clorox bleach, for 10 min. Incubate the electrodes in ddH_2O to remove excess hypochlorite solution and left air dried.
▲ **CRITICAL** The hypochlorite solution forms/replenishes a silver chloride layer on the electrode surface. If the silver chloride layer is depleted, the toxic Ag^+ ions leak into the ACSF and internal solution. This can poison the tissue and affect the cell health. Moreover, a silver electrode depleted of silver chloride layer will result in unstable recordings, which is commonly manifested as voltage drifts over the course of tens of minutes. It is, therefore, prudent to clean and recoat the electrodes once a week.

Procedure

Calibrate laser power

● **TIMING ~30 min for calibration only and ~1 day if new optical components need to be installed and laser beam needs to be realigned**

1. Switch on the femtosecond laser and wait for it to stabilize. Keep the laser shutter closed.
   ▲ **CAUTION** Mode-locked lasers produce 100–200 fs pulses with peak power on the order of several 100 kW (compared with a few milliwatts for confocal microscopy). A stray laser beam may, thus, quickly cause irreversible damage to the retina or burns to the skin. Laser safety training and other precautions must be taken. For instance, wear laser safety goggles when working with the beam path.
2. The laser power can be manually attenuated using a polarizing beam splitter and half-wave plate (Fig. 3). Alternatively, a semiautomated system can be created with the polarization rotation controlled by a motor.
   ▲ **CAUTION** A beam dump should be placed to collect the rejected laser beam from the polarizing beam splitter.

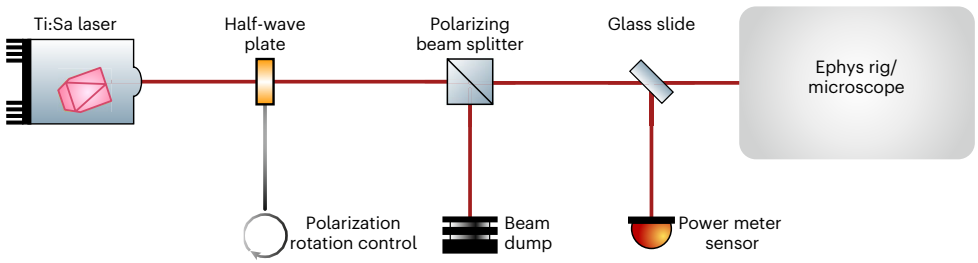

Fig. 3 | Using polarizing beam splitters to control laser power. By combining a half-wave plate with a polarizing beam splitter, a simple laser intensity controller can be constructed. The half-wave plate (also known as a half-lambda or $\lambda/2$ plate) rotates the polarization plane of linearly polarized light, hence turning the orientation of the half-wave plate (for example, using a torsion cable, a rigid rod or a motor) changes the laser light polarization. The polarizing beam splitter allows light of a specific polarization to pass through while rejecting the orthogonal orientation. This combination therefore provides a convenient way to attenuate the laser power before it enters electrophysiology (ephys) rig and microscope. A glass slide added to the beam path reflects a small portion of the laser light onto the active surface of a power meter diode, which acts as a proxy for the overall laser power. The beam dump is a safety measure to collect the rejected laser light. Note that if no beam dump is used, then the rejected light could be fed to another microscope, in which case the half-wave plate and beam splitter combo serves to variably share a laser beam across two setups. This scenario would benefit from adding two more half-wave plate and beam splitter combos downstream to separately regulate the laser power of the two individual rigs.

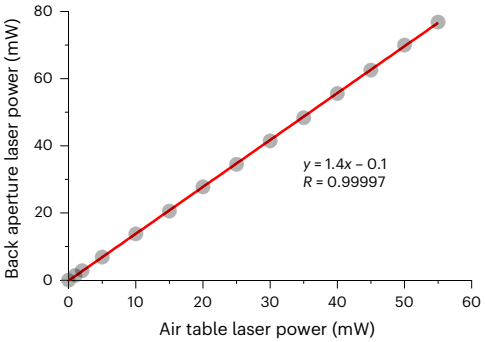

Fig. 4 | Air table laser power is a good proxy for objective back aperture laser power. As indicated by the goodness of fit, *R*, laser power readings at the air table and back aperture correlate strongly (gray circles). The desired back aperture power can, therefore, be set by changing the air table laser power with a polarizing beam splitter and half-wave plate. This provides a convenient way to adjust laser power during experiments. The red line represents the linear regression.

3. Place a glass slide in the beam path and install a laser power meter sensor to pick up the reflected beam. This acts as a proxy that is proportional to the laser power, which we refer to as 'air table laser power' hereafter (Fig. 3).
4. Verify that the laser beam is aligned.
5. Place a laser power meter sensor at the objective back aperture.
6. Open the laser shutters to allow the beam to reach the objective.
7. By changing the laser attenuation in small increments (set up in Step 2), record the laser power readings both at the air table (Step 3) and at the back aperture (Step 6).
   ▲ **CRITICAL STEP** The output power of tunable lasers depends on the wavelength. Therefore, make sure the desired wavelength is selected for calibration. We found that 780 nm is effective for laser axotomy, and this wavelength furthermore excites both Alexa 488 and 594 to permit imaging.
8. Plot a graph of back aperture laser power versus the air table laser power (Fig. 4). Verify the linear correlation with Pearson correlation coefficient; it should be close to 1 (Fig. 4).
9. Extract the linear equation, where y = slope × x + intercept. Using this equation and the laser attenuation controller, set the back aperture power by changing the air table laser power during experiments. For a semiautomated system, this provides a calibration for the laser power control.

Find neuronal connection

● **TIMING ~1.5 h for acute brain slice preparation and recovery and ~20 min for simultaneously patching two to three cells**

10. Prepare acute brain slices as detailed in 'Materials'.
    ◆ **TROUBLESHOOTING**
11. Fill the patch micropipettes with internal solutions and mount on micromanipulators. Apply positive pressure to prevent clogging and for visualizing cell dimple as a health assessment during patching (see Step 14). For detailed information on brain slicing, patching and multiple whole-cell recordings, see previous guides[44,45].
    ◆ **TROUBLESHOOTING**
12. Fill the axon stimulation micropipettes with ACSF and mount on micromanipulator. Apply positive pressure to prevent clogging.
13. Lower all micropipettes to ~200 µm above the slice surface.
14. Using diagonal movement only, form a gigaohm seal with the first target cell. A high-contrast dimple is typically observed on the surface of healthy target cells before releasing positive pressure.
    ◆ **TROUBLESHOOTING**
15. Repeat Step 5 to form gigaohm seals between the patch pipettes and the target cells. To maximize the chance of finding connected cells, sampling cells that are in close proximity (that is, <100 µm) is recommended[49,50]. Patch the deepest cell first and then the shallower ones to minimize seal disruption.
    ◆ **TROUBLESHOOTING**

16. Break through to establish whole-cell configuration with all target cells in quick succession.
◆ TROUBLESHOOTING
17. Assess the neuron health from cell properties such as membrane potential and input resistance.
18. Stimulate the cells to evoke action potentials. A 5-ms-long 1.3 nA current pulse typically works well. For multiple cells, stagger the evoked spikes in patched cells by >500 ms to avoid unintentional induction of long-term plasticity.
19. Assess the recording quality from series resistance indicators such as distorted test pulses and broadening of spike widths.
◆ TROUBLESHOOTING
20. Average traces from 10 to 20 trials and examine the presence of millisecond-coupled postsynaptic response after evoked action potential.
21. When a connection is found, establish a stable baseline by recording for >10 min.
◆ TROUBLESHOOTING

Establish target axon stimulation

● TIMING ~20–30 min

22. Identify the presynaptic cell with two-photon laser microscopy.
23. Capture *z*-stack images of both above and below the cell body with 2 µm *z*-intervals. Typically, a back aperture power of <10 mW is sufficient.
◆ TROUBLESHOOTING
24. Using image software such as FIJI, go through the *z*-stack to find the axon of the presynaptic cell. Identify an axon portion that is ~20 µm from the cell body. Finding the axons can be aided by prior knowledge of their general projection patterns, such as from high-resolution morphometry and axon immunostaining (for example, TUJ1 (also known as βIII-tubulin) or tau). Axons, especially for higher order branches, are typically thinner than dendrites and project further away from the soma (Fig. 5a), accompanied by more complex arborization (gray arrows in Fig. 5b). While dendrites typically branch in a fan-out pattern, axons often branch back on themselves (pink and red arrows in Fig. 5c). For layer 2/3 and layer 5 pyramidal cells in the neocortex, a key identifier is that their main axons project toward and join the white matter below layer 6 (white arrows in Fig. 5a), with axon collaterals (primary axon branches) often, though not always, branching off almost orthogonal to the main axons (green arrow in Fig. 5c). This contrasts with basal dendrites, in which branches are typically seen forking out at ~30°. Some but not all dendrites may also contain dendritic protrusions such as filopodia and spines (blue rectangle in Fig. 5c). While the diameters of dendrites remain similar, the main axon stemming from the cell soma tapers quickly. Combining all the above features helps the experimenter to quickly identify the axon. As axons are also highly excitable, the stimulation steps below can help further confirm that the axon is targeted.
25. Guided by live two-photon laser imaging, position the axon stimulation electrode ~1 µm away from the desired axon portion (Fig. 6a–c). Before entering the slice, release positive pressure and use only diagonal movement for positioning the pipette.
◆ TROUBLESHOOTING
26. Apply a train of five 100 µs biphasic stimulation at 30 Hz, with each train following a voltage ramp from 0 to 18 V in 2 V steps at 1 s inter-ramp intervals (Fig. 7).
27. Examine the presence of antidromic action potentials recorded with the presynaptic cell pipette and postsynaptic responses with the postsynaptic cell pipette (Fig. 7).
◆ TROUBLESHOOTING
28. Repeat the ramp three to five times to identify a consistent minimum stimulation voltage threshold needed to evoke action potentials and postsynaptic responses.
29. Using 120% of the minimum stimulation voltage, evoke action potentials with the normal experimental protocol and record postsynaptic responses (Fig. 6d).
30. Observe the time course to ensure the stability of the recording for at least ~10 min.
◆ TROUBLESHOOTING
31. (Optional) Move on to two-photon laser axotomy as Step 30 is being carried out to save time.

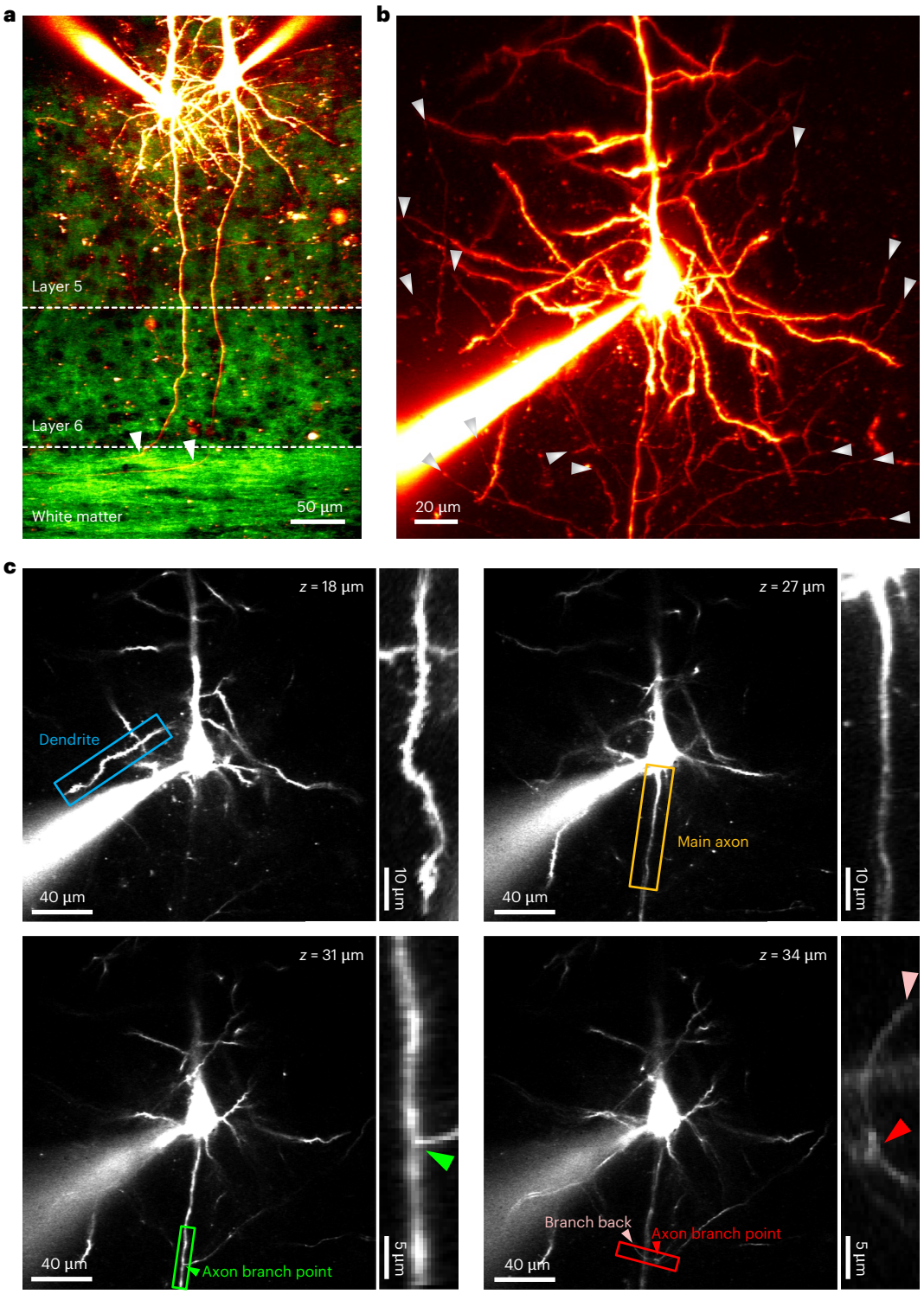

Fig. 5 | Identifying the axon. a, Two sample layer-5 pyramidal cells (red) whose axons traverse layers 5 and 6 to reach the white matter (white arrows). **b**, Close-up of a layer-5 pyramidal cell, to aid visualization of thin processes. Some axon arbors are indicated by the gray arrows. Compared with the dendrites, note the characteristically complex axonal arborization pattern and the relatively small axon diameter. **c**, Single *z* planes of the same cell in **b** and enlarged portions of their respective rectangles. The dendrites have relatively large diameter, with characteristic dendritic protrusions known as spines (blue rectangle). By contrast, the main axon tapers quickly from the soma to form quite thin compartments (orange rectangle). Even thinner primary axon branches tend to branch off at right angle from the main axon (green box and arrow). Axons also often branch back toward the soma (red box, red and pink arrows), which dendrites rarely do.

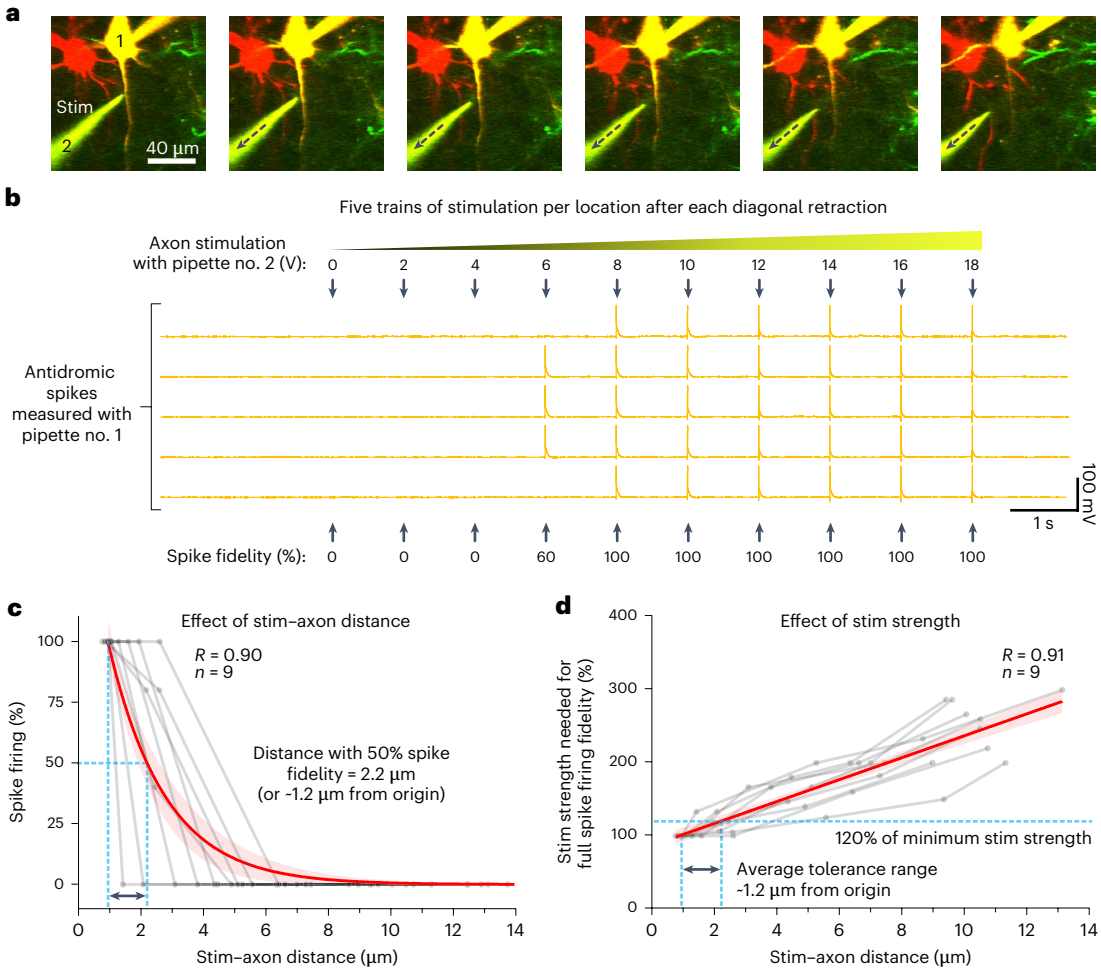

Fig. 6 | Achieving high spike fidelity by optimizing stimulation distance and strength. a, To measure how the stimulation distance and strength affect axon-evoked spike fidelity, the axon stimulation pipette (stim; dotted arrow) was progressively retracted. Note that the pipette was diagonally retracted, which is represented by focusing on the *z* plane where the pipette tip was positioned. **b**, At each stimulation pipette location (that is, pertaining to stim distance from the axon), a single stimulation each in a voltage ramp of 0–18 V in 2 V steps was applied with 1 s interstimulation intervals (pipette no. 2). The stimulation ramp was repeated five times, and the success rate of spike firing was tallied for each stimulation strength (measured as antidromic spike with pipette no. 1). **c**, As the stim–axon distance increased, the spike firing success rate dropped. An exponential decay function was fitted by the red line, with 95% confidence intervals in pink. Spike firing success rate dropped to 50% when the stimulation pipette was moved ~1.2 µm away from the origin (*n* = cells). This indicates that by using the minimum stimulation strength at origin, the axon stimulation is specific to <1.2 µm of the original pipette position, which ensures the specificity of the protocol. **d**, As the stim–axon distance increased, the stimulation strength required for full spike firing fidelity also increased. A linear function was fitted by the red line, with 95% confidence intervals in pink; 120% of minimum stimulation voltage provides an average spatial tolerance of ~1.2 µm from the stimulation origin (*n* = cells). To prevent recordings being interrupted by minor tissue drifts and to ensure axon-evoked spike fidelity, 120% of minimum stimulation voltage is therefore recommended. Adapted from ref. 16, CC BY 4.0 (https://creativecommons.org/licenses/by/4.0/).

Two-photon laser axotomy

● **TIMING ~5–10 min**

32. Identify an axon position ~5–10 µm away from the cell body.
33. Move the center of the two-photon microscopy field of view to the desired axon position, with the focus on the brightest *z* plane.
    ◆ **TROUBLESHOOTING**
34. Close the laser gating shutter.

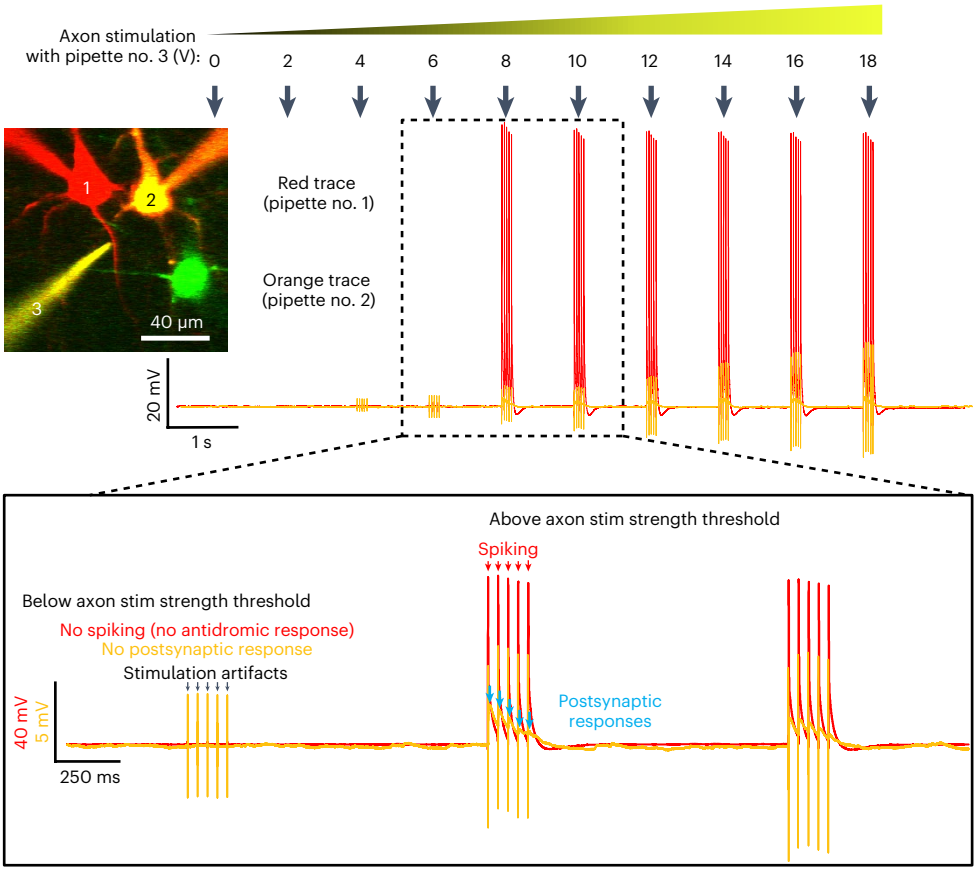

Fig. 7 | Identifying minimum stimulation strength. After the axon stimulation pipette (no. 3) was guided to ~1 µm from the axon, five stimulation each in a voltage ramp of 0–18 V in 2 V steps was applied with 1 s interstep intervals. Three to five repeats were employed to identify the minimum stimulation voltage threshold required for evoking spikes reliably (measured as antidromic responses with somatic pipette no. 1; red arrows). Millisecond-coupled axon-evoked postsynaptic responses (measured with somatic pipette no. 2; blue arrows) should only be observed when the minimum threshold for triggering spike firing is reached. Adapted from ref. 16, CC BY 4.0 (https://creativecommons.org/licenses/by/4.0/).

35. Increase the laser power to 50 mW at back aperture.
36. Set up a 5 s long electrophysiology protocol that evoke action potentials at 120% of the minimum stimulation voltage with a 2 s delay from the start.
37. Using the electrophysiology recording software as a trigger, perform a 4 × 2 µm (width × height) sine-square cut at 125 Hz for 500 ms every 10 s.
    ◆ **TROUBLESHOOTING**
38. Observe the electrophysiology properties of the cells to assess if the axotomy is successful. Terminate the axotomy protocol when the axotomy signatures are found (Fig. 8). A median of four laser cuts were needed in our experience ($n = 39$).
    ▲ **CRITICAL** A successful isolation of the axon from the cell body is crucial for assessing compartmentalized signaling. Several key parameters aid the identification (Fig. 8c). First, the antidromic action potential measured with presynaptic pipette should be attenuated. Second, the stereotypical rapid depolarization of presynaptic soma and simultaneously input resistance drop should be observed.
39. (Optional) Repeat Step 40 and Step 41 until axotomy signatures are seen. This ensures that the tissue and the target axon only receive the minimal amount of laser exposure.

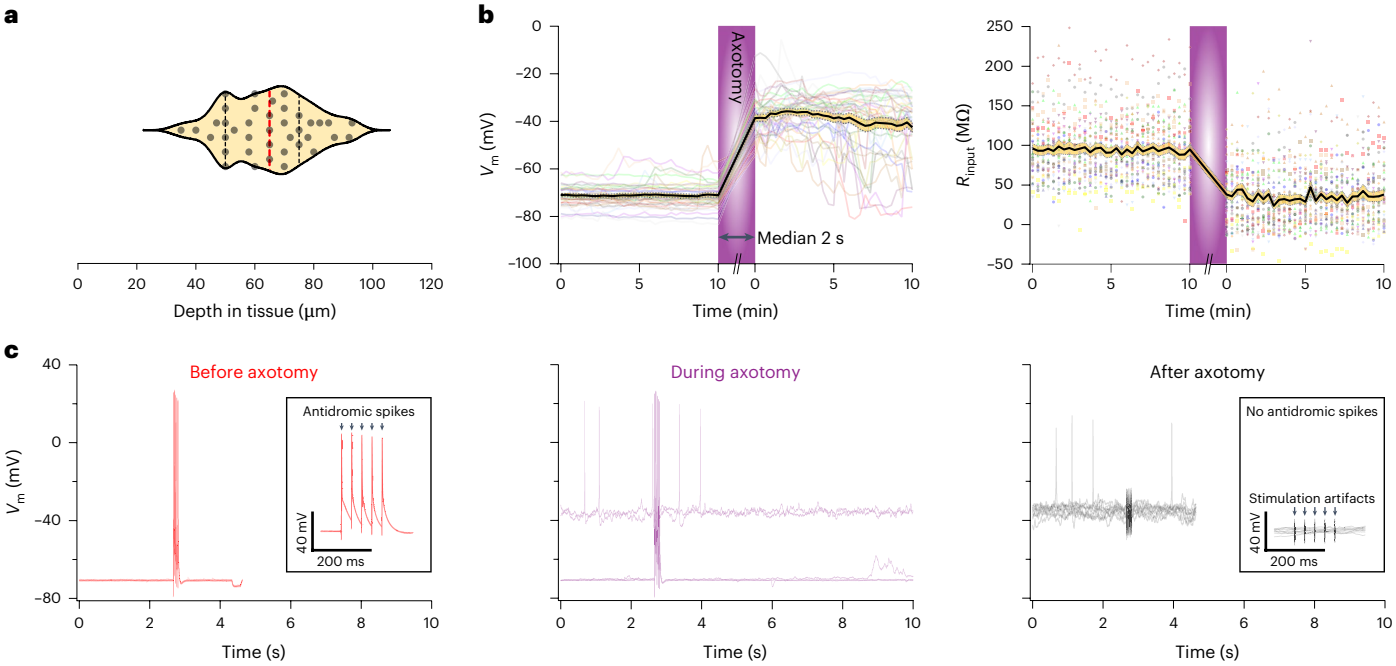

Fig. 8 | Successful axotomy is identified by distinct changes in electrophysiology properties. a, Laser axotomy was successfully performed at different depths in the tissue and was effective down to a depth of at least ~100 μm. With the two-photon laser tuned to 780 nm and a back aperture power of 50 mW, a unit of 500 ms laser cut was performed every 10 s. The axotomy procedure was terminated when antidromic action potential was attenuated. The red dotted line indicates the median while the black dotted lines indicate the 25% and 75% quartiles ($n = 39$ cells). **b**, Successful laser axotomy was also accompanied by rapid depolarization of membrane potential (V_m) and reduced input resistance (R_{input}). Individual V_m and R_{input} traces are multicolored, while the average is in black with standard error of the mean as the orange shade. The median axotomy time was 2 s ($n = 39$ cells). In 12 out of the 39 cells, the voltage ramps were recorded without the test pulses needed for the R_{input} measurement, so were omitted here. Adapted from ref. 16, CC BY 4.0 (https://creativecommons.org/licenses/by/4.0/). **c**, Sample experiment showing the presynaptic cell recordings before (ten traces), during (five traces) and after axotomy (ten traces). Before, the antidromic spikes were reliably recorded from cell soma when action potentials were evoked with axon stimulation. During and after a successful axotomy, the attenuation of antidromic spikes was accompanied by rapid depolarization of the cell soma (from ~−75 mV to ~−40 mV). The insets focus on the time periods when the axon was stimulated; note that the stimulation artifacts and not antidromic spikes were seen after axotomy.

40. (Optional) Observe the axon cut with two-photon microscopy. It is worth noting that our axotomy protocol has micrometer precision (Fig. 9), so the cut may sometimes be hard to see unless a *z*-stack is acquired. The appearance of a gap or sometimes blebs between the cell body and axotomized axon may also take tens of minutes. The electrophysiology signatures are thus more accurate and offer real-time experimenter feedback.

Electrophysiology recording of connection with isolated axon

● **TIMING ~1 h**

41. Using 120% of the minimum stimulation voltage, evoke action potentials with the normal experimental protocol to record postsynaptic responses. Continue to monitor for the lack of antidromic action potentials to ensure axotomized axon remains isolated from the cell soma.
42. Observe the postsynaptic responses, which on average recover and reach stability ~15 min after axotomy (Fig. 10).
43. Establish a stable baseline by recording for 10–20 min.
    ◆ **TROUBLESHOOTING**
44. (Optional) Wash-in drugs to observe changes in neurotransmission and synaptic properties.
45. (Optional) Induce long-term plasticity to observe changes in neurotransmission and synaptic properties.

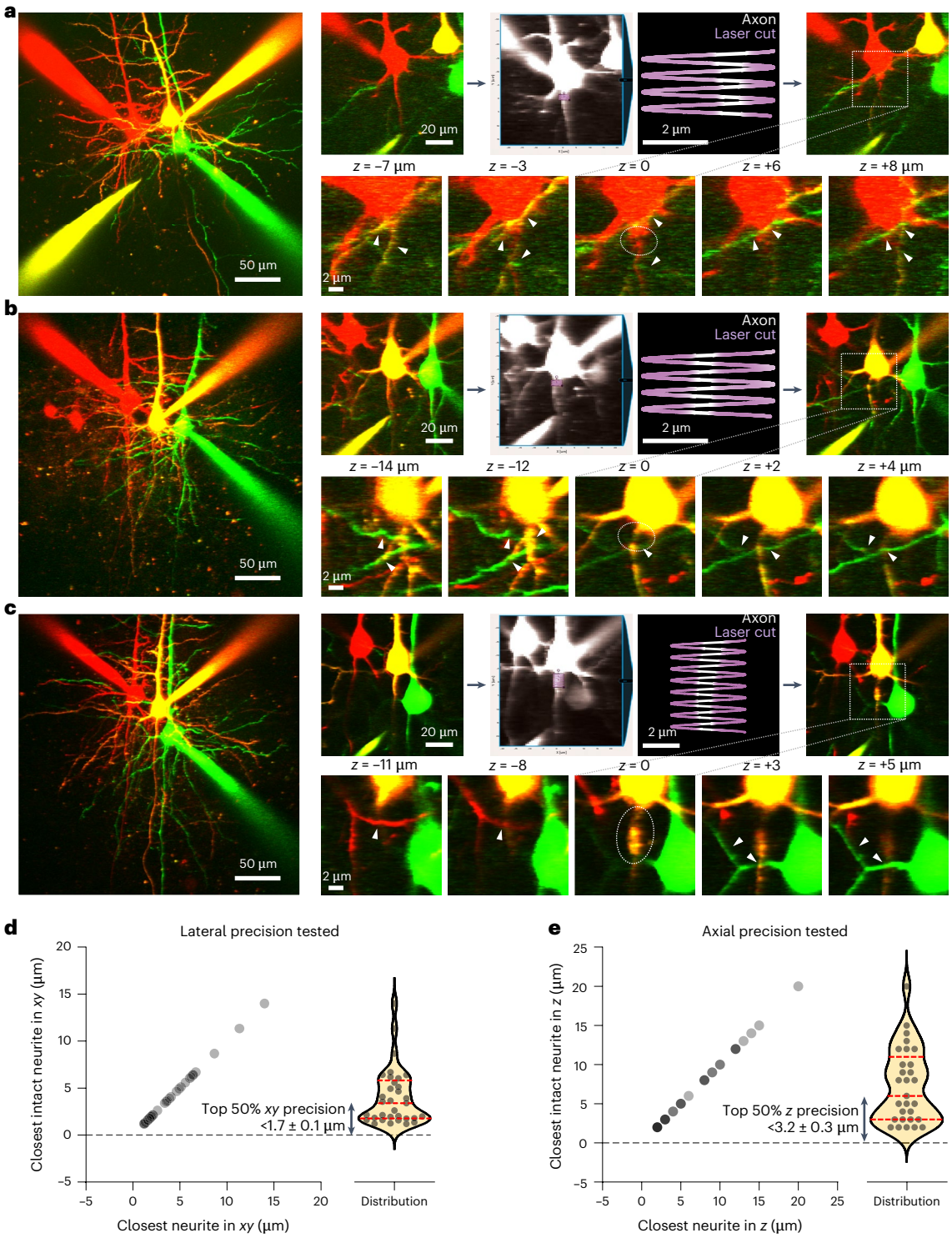

Fig. 9 | Two-photon laser microsurgery has micrometer precision. a, In a sample triplet-recordings, the cell in red was targeted for 4 µm × 2 µm sine-square axotomy. The dotted area is enlarged in the second row. Dashed circle highlights the site of axotomy. Note the neurites within microns in the *x*, *y* and *z* planes (white arrow heads) were intact after axotomy. **b**, Same as **a** with cell in orange targeted for 4 µm × 2 µm sine-square axotomy. **c**, Same as **a** with cell in orange targeted for 4 µm × 5 µm sine-square axotomy. Adapted from ref. 16, CC BY 4.0 (https://creativecommons.org/licenses/by/4.0/). **d**, Empirical test of lateral precision. The neurite closest to laser surgery site in the *xy* plane for all samples were intact, observed at 61.0 ± 3.7 min postsurgery ($n = 33$) (median = 3.4 µm, minimum = 1.2 µm, mean precision of top 50% = 1.7 ± 0.1 µm). **e**, Empirical test of axial precision. The neurite closest to laser surgery site in the *z* plane for all samples were intact, observed at 60.7 ± 3.7 min postsurgery ($n = 30$) (median = 6 µm, minimum = 2 µm, mean precision of top 50% = 3.2 ± 0.3 µm). The red dotted lines represent 75% quartile, median and 25% quartile, respectively, from top to bottom.

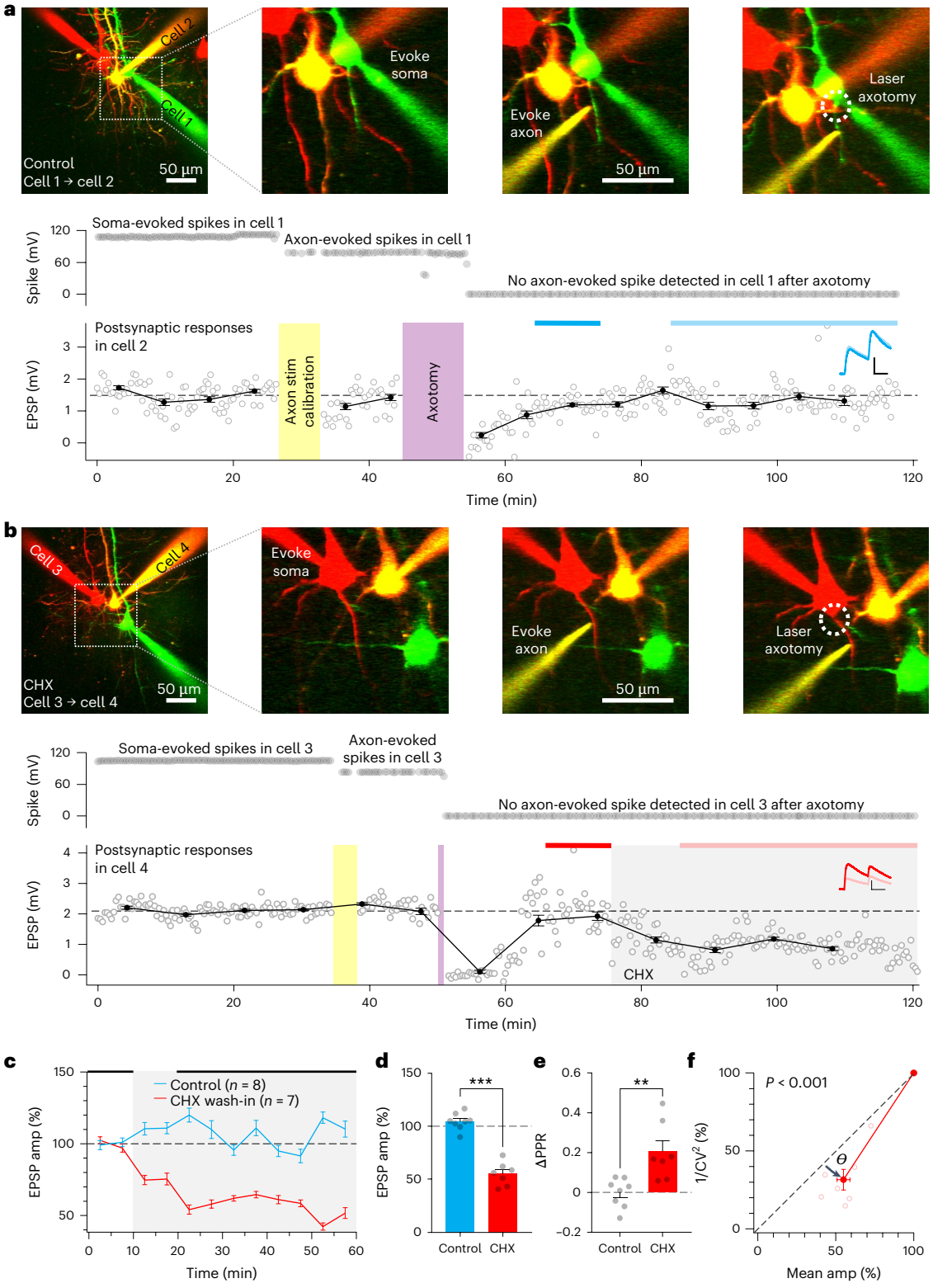
a
Cell 2
Cell 1
Control
Cell 1 → cell 2
50 µm
Evoke soma
Evoke axon
50 µm
Laser axotomy
Soma-evoked spikes in cell 1
Axon-evoked spikes in cell 1
No axon-evoked spike detected in cell 1 after axotomy
Spike (mV)
Postsynaptic responses in cell 2
Axon stim calibration
Axotomy
EPSP (mV)
Time (min)
b
Cell 3
Cell 4
CHX
Cell 3 → cell 4
50 µm
Evoke soma
Evoke axon
50 µm
Laser axotomy
Soma-evoked spikes in cell 3
Axon-evoked spikes in cell 3
No axon-evoked spike detected in cell 3 after axotomy
Spike (mV)
Postsynaptic responses in cell 4
CHX
EPSP (mV)
Time (min)
c
Control (n = 8)
CHX wash-in (n = 7)
EPSP amp (%)
Time (min)
d
***
EPSP amp (%)
Control
CHX
e
**
ΔPPR
Control
CHX
f
P < 0.001
θ
1/CV² (%)
Mean amp (%)

Fig. 10 | Sample experiments with two-photon laser axotomy. a, Control experiment shows establishment of axon-evoked spikes and corresponding excitatory postsynaptic potentials (EPSPs), followed by no presynaptic spike after axotomy, yet presence of EPSPs due to spiking isolated axon. Blue traces and periods show stable synaptic responses. **b**, Within minutes, the translation blocker CHX reduced EPSPs (red traces and periods) elicited by stimulation of isolated axon. **c**, EPSP amplitude (amp) weakened postaxotomy with but not without CHX (n = connections). This revealed that axonal but not somatic protein synthesis affected release. **d**, CHX reduced postaxotomy EPSPs compared with controls. **e**, Analysis of PPR. **f**, CV (Wilcoxon test, $\theta = 11° \pm 2°$, $P < 0.001$) agreed that CHX reduced presynaptic release (Student's t-test for (**d**,**e**); $^{**}P < 0.01$, $^{***}P < 0.001$). The error bars represent the standard error of the mean. Scale bars for traces, $y = 0.8$ mV and $x = 20$ ms. Adapted from ref. 16. CC BY 4.0 (https://creativecommons.org/licenses/by/4.0/).

Troubleshooting

Step	Problem	Possible reason	Solution
10, 14, 15, 16, 43	Bad brain slice and cell quality	Tissue degeneration	Speed up dissection and slicing, aim to finish within 15 min
			Allow ACSF to cool down to almost 0 °C before beginning dissection and slicing. An alternative is to put fresh ACSF in the −20/−80 °C freezer to make a ACSF slush
			Lower the $CaCl_2$ to 1 mM and raise $MgCl_2$ to 2 mM for dissection, slicing and recovery. This is recommended for mouse older than postnatal day 16
			Perform slicing with a high-quality slicer, with minimal blade vibration along the vertical axis
		Severed neuronal processes during slice preparation	Research on the orientation of neuronal processes in the system of interest. Arrange the brain tissue such that the neuronal processes are approximately parallel to the cutting plane. The result can be verified with contrast-enhanced microscopy, which allows neuronal processes to be traced and facilitate healthy cell selection
		Presence of detergents, which may dissolve the lipid-rich cell membrane	Separate labware for electrophysiology from those for other experiments. Never use detergent to clean. Most electrophysiology solutions are mild and nonsticky, meaning repeated rinsing with ddH_2O is sufficient. Use 70% ethanol if necessary
		Incorrect osmolality of solutions	Calibrate the osmometer to ensure proper functioning. Measure and adjust osmolality of solutions to the correct range. Incorrect osmolality often results in cells being bloated or shriveled up
		Toxicity from the bare silver of electrodes	Regularly recoat the electrodes with 6% sodium hypochlorite solution. This ensures the presence of a silver chloride layer on the electrode surface
11	Air bubbles trapped in internal solution inside micropipette, which could cause electrical discontinuity between the electrode and internal solution	Air bubbles introduced during pipette filling	When using a microfil or microloader tip to load the internal solution, progressively pull out the tip to match the solution front in the micropipette
			Gently flicker the loaded micropipette to remove remaining bubbles
14	Hard to form gigaohm seal	The micropipette is clogged internally	Refilter the internal solution. Make sure the tube used for the filtered solution is clean and free of manufacturing faults. We had an experience where microcentrifuge tubes came containing micro fibrils, which were only visible under high magnification
		The micropipette is blocked from the outside	Use high-quality ddH_2O and reagents, and clean containers to prepare ACSF. Filtering is generally not needed. Dirt/salt deposits can also come from the perfusion system, which can be cleaned by first running through ~100 mL 70% ethanol or ~20 mL 0.5 M HCl, followed by ddH_2O. Changing the perfusion tubing quarterly is also recommended. The pipette may also be blocked by cell debris, which can be prevented by careful maneuver of micropipettes. The micropipettes should never touch the tissue before being directed to patch a cell. If this happens by accident, change to a new micropipette
		Incorrect osmolality of solutions	See troubleshooting for Step 13, 17, 18, 19, 46
		The opening of the micropipette is too big	Calibrate the micropipette puller program. Typically, increasing the pull velocity and heat would help shaping a smaller tip, making it easier to be sealed by the membrane
15	Targeting of the subsequent cell disrupts the previous seals	The slice is being dragged while the micropipettes that have already formed a seal stay static	Use only diagonal movement for patching to minimize the dragging. When the tissue moves, gently reposition the pipettes to where the initial seal was formed
		The positive pressure applied when approaching the target cell is too high, causing cells to be dislodged	Reduce the positive pressure. Alternatively, use a manometer to standardize the pressure applied. 3–4 Psi or 0.25 bar is a good initial point for this system-specific calibration

Troubleshooting (continued)

Step	Problem	Possible reason	Solution
		The micropipette drifts	Properly secure the micropipettes on the micromanipulator. We recommend clamping the pipettes by the glass directly instead of the pipette holders. This reduces the pivoting motion of pipette
		The opening of the micropipette is too big	See troubleshooting for Step 17
16	Does not break through	The opening of the micropipette is too small	Calibrate the micropipette puller program. Typically, decreasing the pull velocity and heat would help shaping a bigger tip, making it easier to break through the sealed membrane
		The seal is not properly formed, that is, not reaching gigaohm	See troubleshooting for Step 17 and 18
		Leaks in pressure tubing	Make sure all the joints and stopcocks are secured and that the tubing system is not leaking. Change these components if in doubt
		Various individual or combinations of issues from above	When the typical brief 0.5 s gentle suction pulses do not work, try longer suction pulses that last 2–3 s each. This can be accompanied by a gradual ramp up of suction within each pulse. If this fails, lock in a small amount of negative pressure in the tubing–micropipette assembly. To prevent cell contents from being aspirated, the locked-in pressure should be released as soon as breakthrough happens. Although not recommended as the first methods to try due to difficulty, nonmechanical breakthrough is also possible. One way is voltage clamping the cell at −140 mV to inject a large current, which must be rapidly switched to current clamp after breaking through to prevent cell damage. A final resort is to use the amplifier 'buzz' function to cause current to oscillate, which can rupture the patch. Yet this method generally leaves the cell unhealthy and should be used sparingly
	Breaks through before applying suction	Bad slice and cell quality, causing leaky cell membranes	See troubleshooting for Step 13, 17, 18, 19, 46
		The seal is mechanically ruptured or poked through before desired timing	See troubleshooting for Step 18
19	Distorted electrophysiology signatures	Series resistance is too high	Calibrate the micropipette puller program. Typically, decreasing the pull velocity and heat would help shaping a bigger tip, making access better to reduce series resistance
21	Unstable recording	High noise introduced into recording	Make sure the equipment is properly grounded. The patching rig should be shielded in a Faraday cage to block the electromagnetic field interferences
		The postsynaptic response is small, which can be masked by noise	Set a threshold for the minimum synaptic strength as a quality selection criterion. We found 0.3 mV to be a good cutoff to ensure accurate measurement of signals
23, 33	Beading of neuronal processes or abnormal electrophysiology properties	Phototoxicity	Attenuate the laser to tune down the laser power and/or shorten laser pixel dwell time. The signal can be compensated by increasing the photomultiplier tube gain, loading a higher concentration of fluorescence dye or using optics with high numerical aperture to collect the emitted photons. Averaging multiple images of the same frame also reduces the influence of shot noise
			At high magnifications, the dwell time per unit area may effectively be prolonged. Therefore, the laser power can be lowered and/or the line scan speed can be increased to avoid phototoxicity
			Only shine the laser on samples when necessary. For initial search of the presynaptic axon and distance estimation, take an image stack for examination to minimize laser exposure
25	Losing the patched cells	Targeting the axon disrupts the patched cells, due to tissue movement	See troubleshooting for Step 18
	The fluorescence dye from the axon stimulation pipette obscures the field of view	Residual positive pressure during approaching	Make sure positive pressure is fully released just before entering the slice
	Cannot visualize the axon stimulation pipette tip with two-photon imaging	Dye-filled ACSF gets pulled back into the pipette when the positive pressure is released	Gently apply some positive pressure to push nonfluorescent ACSF out form the tip. Then, release the positive pressure again and stop pressure flow immediately before the pullback happens. It is possible that this needs to be repeated a few times to achieve
17, 30	No responses, possibly after initial responses	The axon is damaged during positioning of stimulation pipette	Restart from Procedure 2. Be mindful that the stimulation pipette should not come into direct physical contact with the target axon. Always have the stimulation pipette staying on one side of the axon and do not cross, as this prevents the axon from being damaged

Troubleshooting (continued)

Step	Problem	Possible reason	Solution
		Vibration on air table displaced the axon stimulation pipette	Use separate air tables for individual setups. Alternatively, perform this experiment when no one else is using the same air table
		Equipment not stable	Clamp down all equipment and secure the pipettes on micromanipulators
		The axon stimulation pipette is filled with internal solution instead of ACSF, leading to incorrect ion concentration gradients locally near the axon stimulation site	Replace the micropipette and correctly fill it with ACSF
	Presence of antidromic action potentials but not postsynaptic responses	Synaptic contacts or postsynaptic cell patch/health compromised	Restart from Procedure 2. See troubleshooting for Step 18
	Consistent antidromic action potentials but vastly different postsynaptic responses	Cells other than the target axon are recruited by the stimulation pipette. This could sometimes manifest as multiple responses with a single spike due to different synaptic latencies	Restart from Step 27 by choosing another axon stimulation position. A few micrometers away can make a big difference
37	Triggering fails	Incorrect wiring between the digital acquisition boards for electrophysiology and imaging	Check the electrophysiology software for the designate port for transmitting the triggering signal. Then, check the imaging software for the designated port for receiving the triggering signal. Wire the correct ports between the electrophysiology and imaging digital acquisition boards. If the designated ports are already in use for other purposes, change the port numbers. This function is available in most software
		Digital acquisition boards become tripped up in an error state, possibly from the experimenter ending acquisition before the commanded protocol has finished	Reset the digital acquisition boards via the software

Timing

Calibrate laser power
Calibration only: 30 min
With installation of custom laser attenuator and power meter diode: 1 day

Find neuronal connection
Acute slice preparation recovery: 90 min
Patch two to three cells: 20 min

Establish target axon stimulation
20–30 min

Two-photon laser axotomy
5–10 min

Electrophysiology recording of connection with isolated axon
1 h

Anticipated results

This protocol combines two-photon laser microsurgery and targeted axon stimulation to examine axonal signaling. By measuring the reliable axon-evoked antidromic action potentials,

this provides a tractable means to isolate the axon with micrometer precision and minimal tissue perturbation.

Here, we provide experiment examples[16]. Figure 10a shows a control experiment where cell 1 is connected to cell 2. After establishing a stable baseline recording, axon stimulation pipette was calibrated to reliably evoke spikes. It is noteworthy that the axon-evoked spike amplitude would appear to be smaller than that of soma evoked. This is because of the voltage drop across the series resistance, which gives the false impression of a contribution to the membrane potential, V_m. By contrast, axon-evoked spikes bypass this problem. Two-photon axotomy was then performed to isolate the cell 1 axon from its soma. After ~10 min, the postsynaptic responses recovered and remained stable for >1 h post-axotomy, indicating a high degree of autonomy in the isolate axon to sustain synaptic release.

Figure 10b shows a similar experimental design as Fig. 10a, with cell 3 connected to cell 4. Instead, the RNA translation blocker cycloheximide (CHX) was washed in, which suppressed neurotransmission (Fig. 10a–d). Analyses of PPR and of CV both suggested that the observed suppression was presynaptic (Fig. 10e,f). Together, the axotomy experiment provided strong support that local protein synthesis in axons sustains release during high-frequency neurotransmission[16]. This provides a new perspective on how neurotransmission and memory are dynamically regulated by protein synthesis.

Postsynaptic signaling has long been dominating health and disease models, leading to an unfortunate bias and a prevailing view that the presynapse has a relatively passive role. This is probably a consequence of the fact that patching postsynaptic cells is easier than patching presynaptic cells, leading to scenario akin to looking for the lost car keys under the streetlight because that is where it is easier to search. Our axotomy method, thus, provides a much-needed tool to uncover hitherto unappreciated forms of presynaptic signaling in brain health and disease.

Data availability

All experimental data are presented as individual data points and are available in both the primary research article[16] and in this protocol. They are also available from the corresponding authors on reasonable request.

Code availability

All custom code used for data acquisition and data analysis are available from the corresponding authors on reasonable request, as well as in the following Zenodo and GitHub links via https://doi.org/10.5281/zenodo.7854025 and https://github.com/pj-sjostrom/MultiPatch.

Received: 3 May 2024; Accepted: 2 December 2024;
Published online: 07 February 2025

References

1. Yuste, R. *Dendritic Spines* (MIT Press, 2010).
2. Braitenberg, V. & Schüz, A. *Cortex: Statistics and Geometry of Neuronal Connectivity* 2nd edn (Springer-Verlag Telos, 1998).
3. Bourne, J. N. & Harris, K. M. Coordination of size and number of excitatory and inhibitory synapses results in a balanced structural plasticity along mature hippocampal CA1 dendrites during LTP. *Hippocampus* **21**, 354–373 (2011).
4. Yang, Y. & Calakos, N. Presynaptic long-term plasticity. *Front. Synaptic Neurosci.* **5**, 8 (2013).
5. Costa, R. P., Mizusaki, B. E. P., Sjöström, P. J. & van Rossum, M. C. W. Functional consequences of pre- and postsynaptic expression of synaptic plasticity. *Philos. Trans. R. Soc. B* **372**, 20160153 (2017).
6. Guzikowski, N. J. & Kavalali, E. T. Nano-organization at the synapse: segregation of distinct forms of neurotransmission. *Front. Synaptic Neurosci.* **13**, 796498 (2021).
7. Chanaday, N. L. & Kavalali, E. T. Presynaptic origins of distinct modes of neurotransmitter release. *Curr. Opin. Neurobiol.* **51**, 119–126 (2018).
8. Wong, H. H., Rannio, S., Jones, V., Thomazeau, A. & Sjöström, P. J. NMDA receptors in axons: there's no coincidence. *J. Physiol.* **599**, 367–387 (2021).
9. Mizusaki, B. E. P., Li, S. S. Y., Costa, R. P. & Sjöström, P. J. Pre- and postsynaptically expressed spike-timing-dependent plasticity contribute differentially to neuronal learning. *PLoS Comput. Biol.* **18**, e1009409 (2022).
10. Costa, R. P., Froemke, R. C., Sjöström, P. J. & van Rossum, M. C. W. Unified pre- and postsynaptic long-term plasticity enables reliable and flexible learning. *eLife* **4**, e09457 (2015).
11. Brock, J. A., Thomazeau, A., Watanabe, A., Li, S. S. Y. & Sjöström, P. J. A practical guide to using CV analysis for determining the locus of synaptic plasticity. *Front. Synaptic Neurosci.* **12**, 11 (2020).
12. Dingman, W. & Sporn, M. B. Molecular theories of memory. *Science* **144**, 26–29 (1964).
13. Frey, U., Krug, M., Brodemann, R., Reymann, K. & Matthies, H. Long-term potentiation induced in dendrites separated from rat's CA1 pyramidal somata does not establish a late phase. *Neurosci. Lett.* **97**, 135–139 (1989).

14. Huber, K. M., Kayser, M. S. & Bear, M. F. Role for rapid dendritic protein synthesis in hippocampal mGluR-dependent long-term depression. *Science* **288**, 1254–1257 (2000).
15. Kang, H. & Schuman, E. M. A requirement for local protein synthesis in neurotrophin-induced hippocampal synaptic plasticity. *Science* **273**, 1402–1406 (1996).
16. Wong, H. H., Watt, A. J. & Sjöström, P. J. Synapse-specific burst coding sustained by local axonal translation. *Neuron* **112**, 264–276.e266 (2024).
17. Markram, H., Gerstner, W. & Sjöström, P. J. A history of spike-timing-dependent plasticity. *Front. Synaptic Neurosci.* **3**, 1–24 (2011).
18. Gomis-Ruth, S., Stiess, M., Wierenga, C. J., Meyn, L. & Bradke, F. Single-cell axotomy of cultured hippocampal neurons integrated in neuronal circuits. *Nat. Protoc.* **9**, 1028–1037 (2014).
19. Aggarwal, A. et al. Glutamate indicators with improved activation kinetics and localization for imaging synaptic transmission. *Nat. Methods* **20**, 925–934 (2023).
20. Marvin, J. S. et al. Stability, affinity, and chromatic variants of the glutamate sensor iGluSnFR. *Nat. Methods* **15**, 936–939 (2018).
21. Marvin, J. S. et al. A genetically encoded fluorescent sensor for in vivo imaging of GABA. *Nat. Methods* **16**, 763–770 (2019).
22. Chen, T. W. et al. Ultrasensitive fluorescent proteins for imaging neuronal activity. *Nature* **499**, 295–300 (2013).
23. Petreanu, L., Huber, D., Sobczyk, A. & Svoboda, K. Channelrhodopsin-2-assisted circuit mapping of long-range callosal projections. *Nat. Neurosci.* **10**, 663–668 (2007).
24. Watt, A. J. et al. Traveling waves in developing cerebellar cortex mediated by asymmetrical Purkinje cell connectivity. *Nat. Neurosci.* **12**, 463–473 (2009).
25. Shigeoka, T. et al. On-site ribosome remodeling by locally synthesized ribosomal proteins in axons. *Cell Rep.* **29**, 3605–3619 e3610 (2019).
26. Cagnetta, R. et al. Noncanonical modulation of the eIF2 pathway controls an increase in local translation during neural wiring. *Mol. Cell* **73**, 474–489 e475 (2019).
27. Cioni, J. M. et al. Axon-axon interactions regulate topographic optic tract sorting via CYFIP2-dependent WAVE complex function. *Neuron* **97**, 1078–1093.e1076 (2018).
28. Wong, H. H. et al. RNA docking and local translation regulate site-specific axon remodeling in vivo. *Neuron* **95**, 852–868.e858 (2017).
29. Levi, G. Ricerche sperimentali sovra elementi nervosi sviluppati in vitro. *Arch. Exp. Zellforsch.* **2**, 244–272 (1926).
30. Shaw, G. & Bray, D. Movement and extension of isolated growth cones. *Exp. Cell Res.* **104**, 55–62 (1977).
31. Hughes, A. The growth of embryonic neurites; a study of cultures of chick neural tissues. *J. Anat.* **87**, 150–162 (1953).
32. Leung, K. M. & Holt, C. E. Live visualization of protein synthesis in axonal growth cones by microinjection of photoconvertible Kaede into Xenopus embryos. *Nat. Protoc.* **3**, 1318–1327 (2008).
33. Harris, W. A., Holt, C. E. & Bonhoeffer, F. Retinal axons with and without their somata, growing to and arborizing in the tectum of *Xenopus* embryos: a time-lapse video study of single fibres in vivo. *Development* **101**, 123–133 (1987).
34. Kretz, A., Marticke, J. K., Happold, C. J., Schmeer, C. & Isenmann, S. A primary culture technique of adult retina for regeneration studies on adult CNS neurons. *Nat. Protoc.* **2**, 131–140 (2007).
35. Song, S., Sjöström, P. J., Reigl, M., Nelson, S. & Chklovskii, D. B. Highly nonrandom features of synaptic connectivity in local cortical circuits. *PLoS Biol.* **3**, e68 (2005).
36. Steinmeyer, J. D. et al. Construction of a femtosecond laser microsurgery system. *Nat. Protoc.* **5**, 395–407 (2010).
37. Ylera, B. et al. Chronically CNS-injured adult sensory neurons gain regenerative competence upon a lesion of their peripheral axon. *Curr. Biol.* **19**, 930–936 (2009).
38. Vandael, D. et al. Subcellular patch-clamp techniques for single-bouton stimulation and simultaneous pre- and postsynaptic recording at cortical synapses. *Nat. Protoc.* **16**, 2947–2967 (2021).
39. Bischofberger, J., Engel, D., Li, L., Geiger, J. R. & Jonas, P. Patch-clamp recording from mossy fiber terminals in hippocampal slices. *Nat. Protoc.* **1**, 2075–2081 (2006).
40. Forsythe, I. D. Direct patch recording from identified presynaptic terminals mediating glutamatergic EPSCs in the rat CNS, in vitro. *J. Physiol.* **479**, 381–387 (1994).
41. Geiger, J. R. & Jonas, P. Dynamic control of presynaptic Ca^{2+} inflow by fast-inactivating K^+ channels in hippocampal mossy fiber boutons. *Neuron* **28**, 927–939 (2000).
42. Larsen, R. S. & Sjöström, P. J. Synapse-type-specific plasticity in local circuits. *Curr. Opin. Neurobiol.* **35**, 127–135 (2015).
43. Chou, C. Y. C. et al. Principles of visual cortex excitatory microcircuit organization. *Innovation* **6**, 100735 (2024).
44. Wong, H. H., Thomazeau, A. & Sjöström, P. J. in *Electrophysiology Book: A Comprehensive Guide for Neurophysiologists* (eds Duguid, I. et al.) (World Scientific Publishing, 2024).
45. Wong, H. H., Camiré, O. & Sjöström, P. J. in *Electrophysiology Book: A Comprehensive Guide for Neurophysiologists* (eds Duguid, I. et al.) (World Scientific Publishing, 2024).
46. Burrone, J., Li, Z. & Murthy, V. N. Studying vesicle cycling in presynaptic terminals using the genetically encoded probe synaptopHluorin. *Nat. Protoc.* **1**, 2970–2978 (2006).
47. Dembrow, N. C. et al. Areal specializations in the morpho-electric and transcriptomic properties of primate layer 5 extratelencephalic projection neurons. *Cell Rep.* **43**, 114718 (2024).
48. Hunt, S. et al. Strong and reliable synaptic communication between pyramidal neurons in adult human cerebral cortex. *Cereb. Cortex* **33**, 2857–2878 (2023).
49. Perin, R., Berger, T. K. & Markram, H. A synaptic organizing principle for cortical neuronal groups. *Proc. Natl Acad. Sci. USA* **108**, 5419–5424 (2011).
50. Holmgren, C., Harkany, T., Svennenfors, B. & Zilberter, Y. Pyramidal cell communication within local networks in layer 2/3 of rat neocortex. *J. Physiol.* **551**, 139–153 (2003).

Acknowledgements

We are grateful to members of the Sjöström and Suvrathan labs for help and useful discussions. H.H.-W.W. was supported by CIHR ICT 193701, CIHR Fellowship 295104, CFREF and McGill HBHL Postdoctoral Fellowship, FRQS Postdoctoral Fellowship 259572 and QBIN Scholarship 35450. A.J.W. received funding from NSERC Discovery grant 2016-05118, CIHR PGs 153150 and 173290. P.J.S. acknowledges funding from CFI LOF 28331, CIHR PG 156223, 191969, 191997, FRSQ CB 254033 and NSERC DG/DAS 2024-06712, 2017-04730 and 2017-507818.

Author contributions

Conceptualization: H.H.-W.W. and P.J.S. Methodology: H.H.-W.W. and P.J.S. Software: P.J.S. Investigation: H.H.-W.W. Writing (original draft): H.H.-W.W. Writing (review and editing): H.H.-W.W., A.J.W. and P.J.S. Funding acquisition: H.H.-W.W., A.J.W. and P.J.S. Supervision: P.J.S and A.J.W.

Competing interests

The authors have no competing interests as defined by Nature Research or other interests that might be perceived to influence the interpretation of the article.

Additional information

Extended data is available for this paper at https://doi.org/10.1038/s41596-024-01125-5.

Correspondence and requests for materials should be addressed to Hovy Ho-Wai Wong or P. Jesper Sjöström.

Peer review information *Nature Protocols* thanks the anonymous reviewer(s) for their contribution to the peer review of this work.

Reprints and permissions information is available at www.nature.com/reprints.

Publisher's note Springer Nature remains neutral with regard to jurisdictional claims in published maps and institutional affiliations.

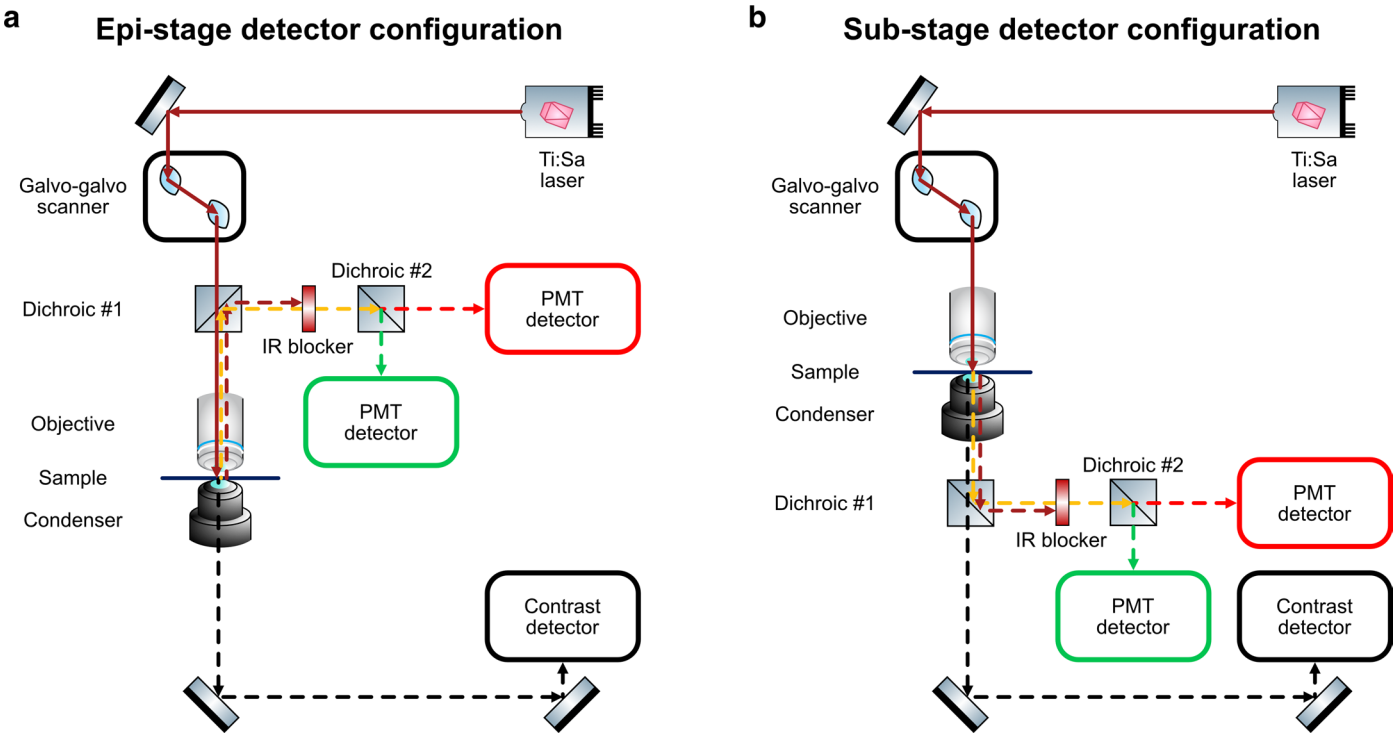

Extended Data Fig. 1 | 2-photon axotomy works flexibly with different microscope designs. a, A setup with epi-stage photomultiplier tube (PMT) detectors. The Ti:Sa laser generates femto-second pulses in the infrared (IR) spectrum. The IR beam is reflected by the galvo-galvo scanner through dichroic #1 and the objective to the sample, where fluorescence is generated by 2-photon excitation. The emitted fluorescence is collected by the objective and reflected by dichroic #1 into the detector assembly. Dichroic #1 thus transmits the IR beam but reflects visible light. The IR-blocking filter between the dichroics ensures that the laser beam does not reach the PMTs. Dichroic #2 splits the emitted fluorescence into red (e.g., RFP or Alexa 594) and green (e.g., GFP or Alexa 480) that is detected by the PMTs. IR transmission through the sample is collected by the condenser and guided to a separate detector, which enables e.g., Dodt contrast or differential-interference contrast. Note that a laser beam in the visible range would be obstructed by Dichroic #1, but this is not true for a femto-second IR beam. **b**, A setup with sub-stage PMTs. Instead of collecting emitted light through the objective, the condenser is used. As the condenser numerical aperture is generally larger than that of the objective, collection efficiency is typically appreciably better with sub-stage PMTs, although both designs can be combined for even better efficiency. Some users rely on substage detectors because Dichroic #1 is after the sample, so it will not block a visible laser beam. However, this consideration is moot for a femto-second IR beam. In conclusion, 2-photon axotomy is readily adaptable to differing 2-photon microscope design.